



## Finite Element Calculation of Field Enhancement in the ASC/UW Magneto-Optical Measurement Setup

P. Bauer<sup>1</sup>, Technical Division, Fermilab  
A. Polyanskii, Applied Superconductivity Center / University of Wisconsin

### 1) Introduction

Finite element (FE) model simulations have been performed to support magneto-optical investigations of high purity niobium (Nb) for superconducting RF cavities conducted at the Applied Superconductivity Center (ASC) of the University of Wisconsin at Madison in collaboration with Fermilab's Technical Division. The magneto-optics studies of small samples of high purity Nb as it is used for superconducting, high gradient RF cavities serves to characterize the superconducting properties of the material. Strong superconducting shielding currents are excited in superconductors in the presence of external magnetic flux. The flux penetration into a type II superconductor, such as Nb, occurs at fields close to the thermo-dynamic critical field,  $H_{c_{therm}}$ . Flux penetration can occur at fields below  $H_{c_{therm}}$  if the superconducting state in the material is weakened, for instance as a result of the presence of a metallic layer on the surface. This is particularly important since it is believed that the penetration of small numbers of flux lines into the cavity surface during RF operation is almost certainly leading to breakdown of the superconducting state. The understanding of DC flux penetration is the first step towards understanding flux penetration in RF fields. Fermilab and the ASC have recently started to collaborate on the magnetic study of the material used in Fermilab's SRF cavities. First results of the magneto-optical investigation of high purity Nb for Fermilab's SRF cavities were recently presented in [1].

Magneto-optics (MO) is a well-developed technique for the characterization of the global (and local) magnetic response of a superconductor. The general aspects of the MO setup at the ASC/UW are described in detail in [2]. MO uses the strong Faraday effect in YFe garnet to measure the vertical magnetic field component above a sample, in this case of superconducting Nb. The garnet is placed on the face of the sample and able to resolve fields of the order of  $1 \text{ mT}$ . The sample shape is typically rectangular or square. Samples with  $5 \times 5 \text{ mm}^2$  or  $3.5 \times 3.5 \text{ mm}^2$  dimensions ( $\sim 1\text{-}3 \text{ mm}$  thick) have been used and these are the geometries that were implemented in the MO models discussed here. Via indirect cooling with a cold finger containing liquid helium, the sample temperature is reduced below the superconducting transition. An external solenoid is used to apply the vertical magnetic field on the sample. Figure 1 shows a schematic of the MO setup as it was implemented in the FE-models. The schematic shows a  $5 \text{ mm}$  wide,  $2 \text{ mm}$  high sample in

---

<sup>1</sup> e-mail: pbauer@fnal.gov

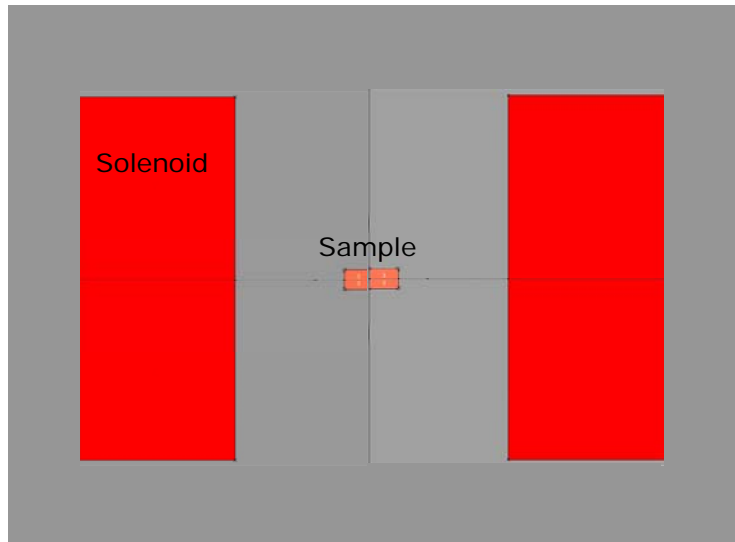


**Figure 1: Schematic of the MO setup as it was implemented in the FE-models.**

the middle of a  $32\text{ mm}$  height solenoid (coil thickness:  $14\text{ mm}$ ). Typically the current density in the solenoid was set to  $10\text{ A/mm}^2$ .

The following discusses the results of the FE modeling of the MO setup. The typical geometry of the MO setup simulated with the FE program OPERA<sup>2</sup>. As shown in Figure 1 the sample and solenoid are surrounded by “vacuum” in the model. As a result of the symmetry of the problem, typically only one quadrant/octant was considered in the 2D/3D models, using the appropriate mirror boundary conditions. The FE modeling serves to predict the field distribution in (and on) the superconducting sample in the “ideal” case. The ideal case is defined as that in which the sample excludes all external magnetic flux. For that purpose the magnetic permeability,  $\mu$ , was set to a very small value ( $\sim 10^{-5}$ ) in the definition of the sample’s material properties. The main output parameters generated by the calculation of the field distribution in and around the sample are –1- the maximum field enhancement factor along the sample edges and –2- the vertical field component on top of the sample in the ideal case (i.e. the case without flux penetration in the sample). The FE model calculations are therefore an important tool for the interpretation of the results of the MO studies.

## 2) 2D Simulation

Figure 2 shows the magnetic flux lines in the MO setup calculated with the OPERA2D model for the case of a superconducting sample with ideal diamagnetism ( $\mu=10^{-5}$ ). The external flux is expelled from the sample, causing flux concentration at the sample’s edges. In Figure 2, which shows only one quadrant of the MO-setup, the field concentration is highest in the upper right corner. Note that the corner of the sample was

<sup>2</sup> OPERA2D and OPERA3D are products of Vectorfields Inc.

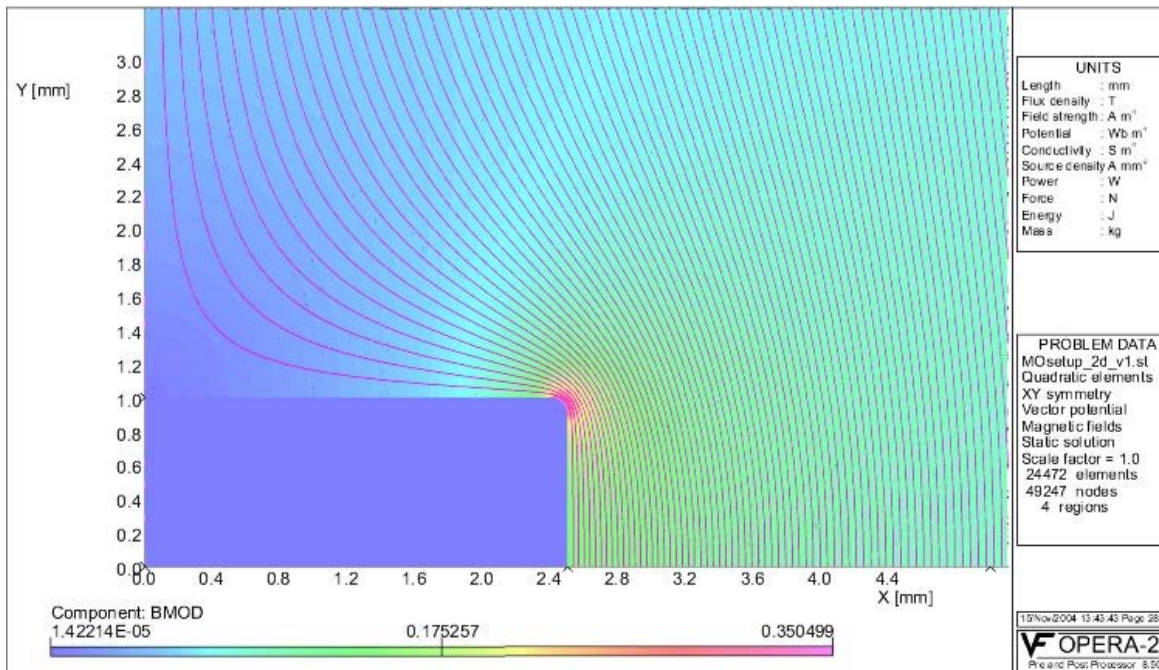


Figure 2: Magnetic field distribution in one quadrant of the MO setup. The sample is perfectly superconducting and excludes all the externally applied flux. The field enhancement is highest at the corner. The corner in the FE model was rounded ( $r=100\ \mu\text{m}$ ).

rounded in the model ( $R=100\ \mu\text{m}$ ), a feature, which is representative of real samples because they undergo strong chemical polishing.

Figure 3 shows the magnetic field on top of the sample ( $y=1.001\ \text{mm}$ ) as function of x-coordinate. The field enhancement at  $x=2.5\ \text{mm}$  (the coordinate of the corner point) is clearly visible. Also shown in Figure 3 is the field profile at a different value of the

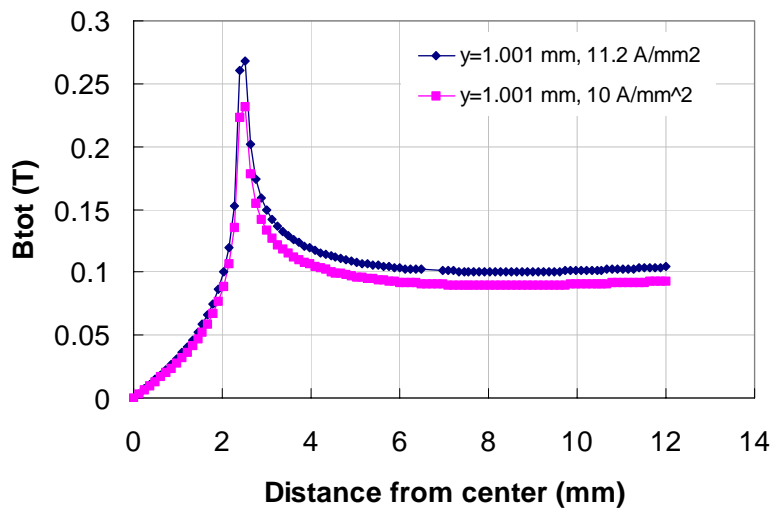
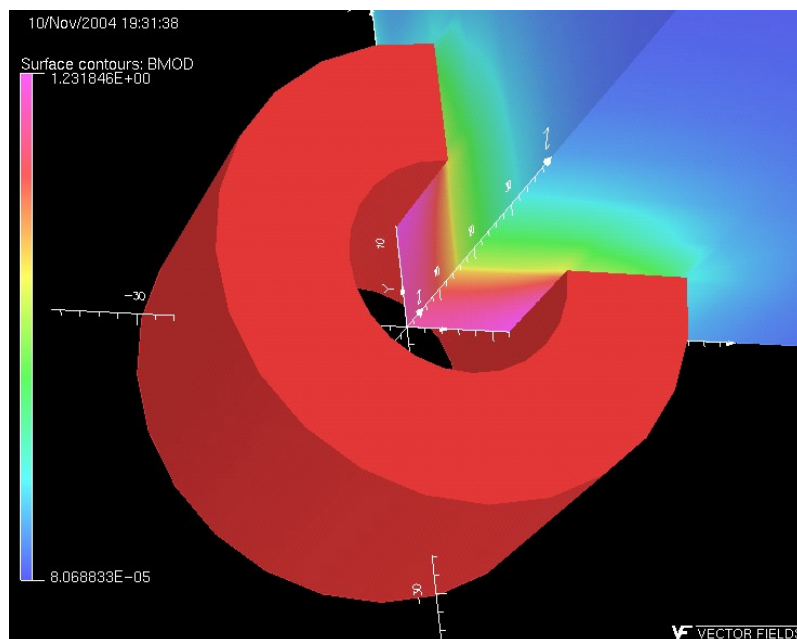


Figure 3: Total field vs distance from solenoid center calculated with OPERA2D for the MO setup (5 mm square, 2 mm thick perfectly diamagnetic sample).

external field (as given by a different current density in the solenoid). The purpose of this comparison is to show that the relative field enhancement in the corner point is independent of the external field strength. The field enhancement factor can be found from the comparison of the magnetic field profile as in Figure 3 with the field profile obtained in the case in which the sample is removed (or the sample is magnetically neutral:  $\mu=1$ ). The field enhancement factor is discussed in further detail in the final chapter of this report. Note that in the case of the MO measurement the field enhancement factor is typically defined with respect to the central field of the solenoid. This procedure is not as precise but more practical because the field in the center of the solenoid is better known than the field at the exact point where the magnetic field peaks (which varies with the sample size of course). The error introduced by this small inaccuracy is at the % level, small enough to be negligible.

### 3) 3D Simulation

For a complete simulation of the ASC MO setup a 3D model is required because of the fact that the sample is rectangular and thus not azimuthally symmetric. Figure 4 shows the 3D model, with the solenoid and a field profile in one octant. The sample in this calculation was assumed to have the properties of vacuum. Therefore the field profile in the bore of the magnet is obviously solenoidal. Figure 5 and Figure 6 show this field profile in further detail. In fact the simulation of the case in which the sample is normal conducting serves as a check of the FE calculation because it can be compared to analytical calculations. Such a comparison, using *Equ. 1*[3] to analytically calculate the magnetic field in the origin, indicates that the FE model is accurate to  $\sim 1\%$ . The parameters  $a_1$  and  $a_2$  in *Equ. 1* stand for the inner and outer radial boundaries of the solenoid and  $b$  is its (total) height. Figure 5 also shows the meshing in the sample and



**Figure 4: Result of 3D calculation of magnetic field in ASC/MO setup with OPERA3D. The sample in this calculation had the “vacuum” properties.**

surrounding area, with the particular feature of rounded corners covered in a finer mesh than the rest of the sample. The mesh is finest in the center, coarsest in the furthest away from the sample.

$$B_z(0,0) = \mu_0 J_{sol} a_1 \beta \ln \left( \frac{\alpha + \sqrt{\alpha^2 + \beta^2}}{1 + \sqrt{1 + \beta^2}} \right), \quad \alpha = \frac{a_2}{a_1}, \quad \beta = \frac{b}{a_1} \quad (T) \quad (1)$$

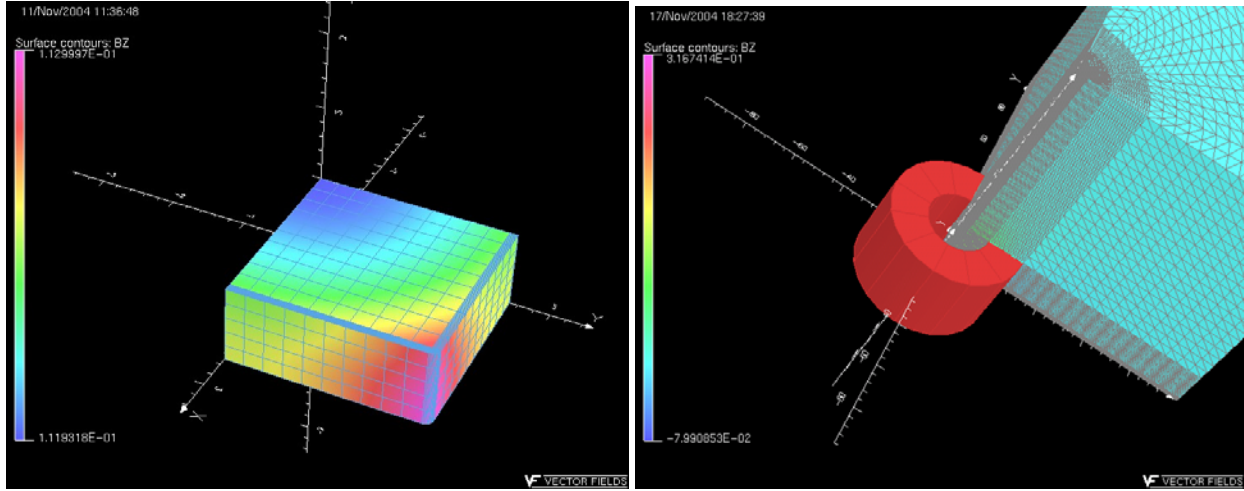


Figure 5: Left: Mesh in sample. Right: Mesh in entire model and solenoid.

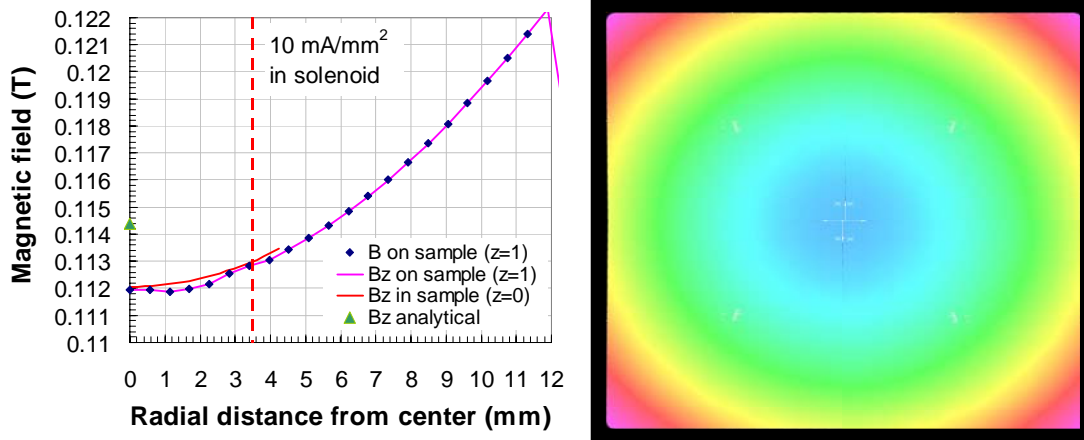


Figure 6: Left: Magnetic field profile across the solenoid bore calculated with OPERA3D (sample in the normal conducting state). Right: Magnetic field strength in mid-plane of entire (normal-conducting) sample.

Figure 7, Figure 8, and Figure 9 show the result of a 3D field simulation for a perfectly diamagnetic sample ( $5 \times 5 \text{ mm}^2$ ,  $2 \text{ mm}$  thickness). The field enhancement on the sample edge is clearly visible.

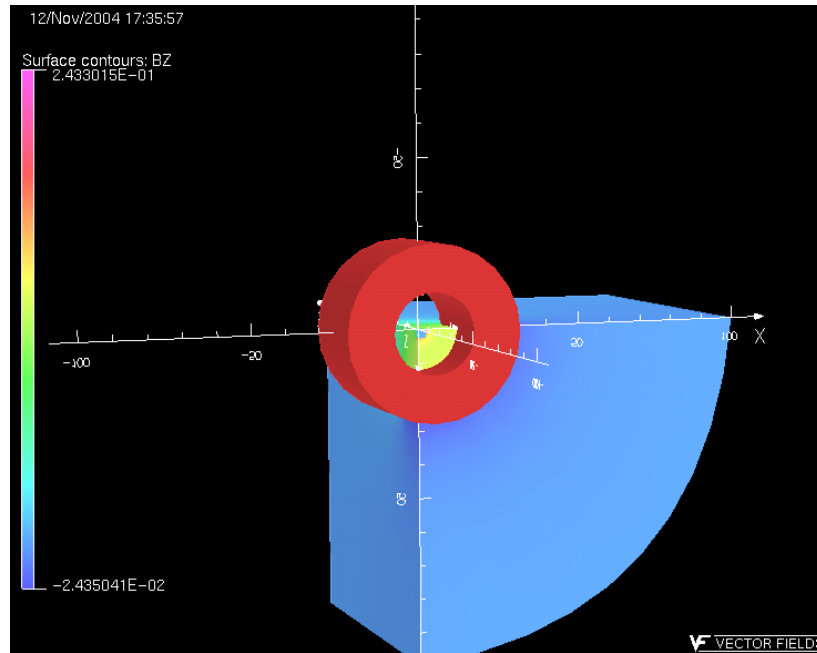


Figure 7: 3D magnetic field in MO setup in the case of a superconducting sample.

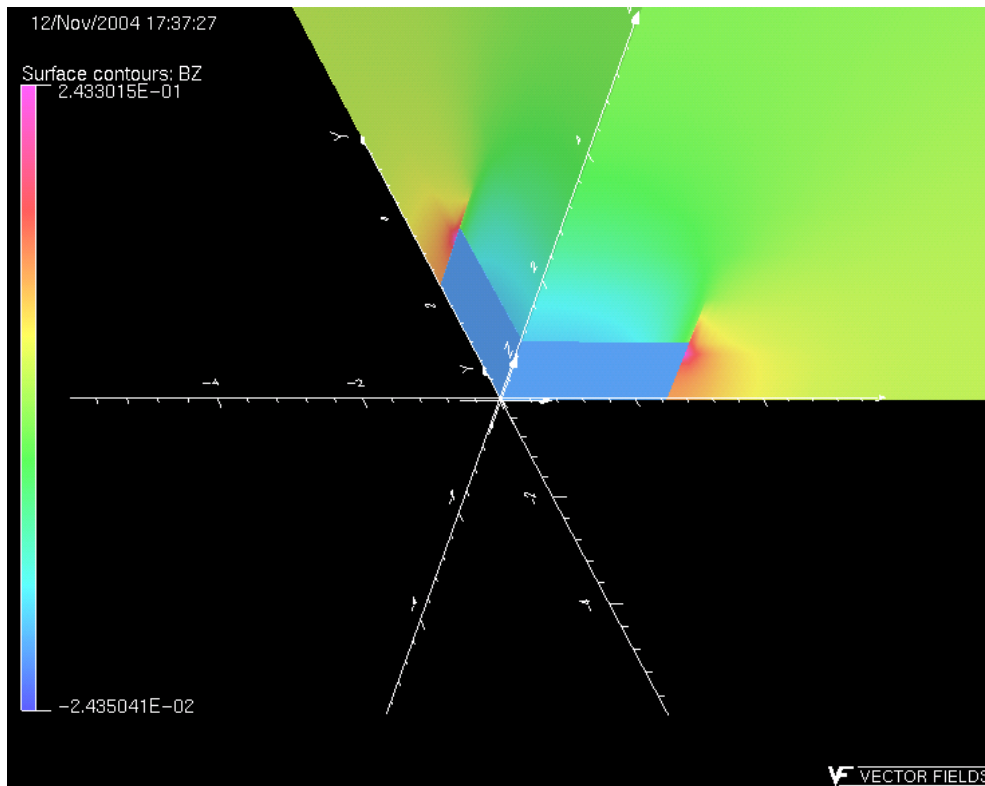
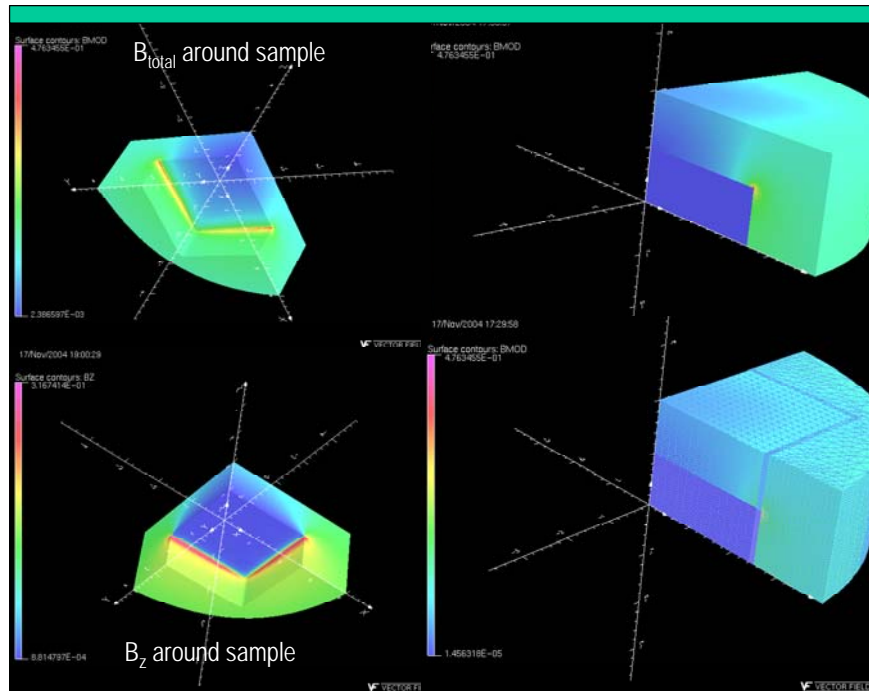
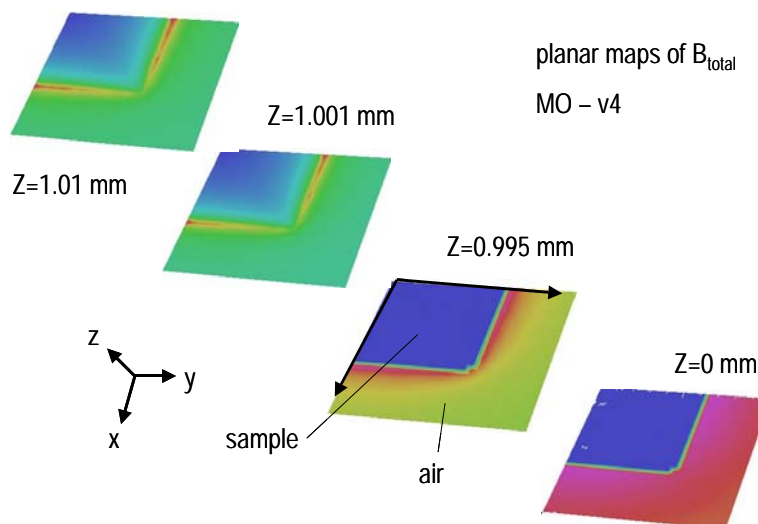


Figure 8: 3D magnetic field in MO setup in the case of a superconducting sample – zoom into sample.



**Figure 9:** 3D magnetic field in MO setup in the case of a superconducting sample. Top: Total field in volume surrounding the sample (first octant). Bottom: Vertical field in volume surrounding the sample. The sample was entirely removed to reveal the fields just outside of its boundaries.

In particular the plot in Figure 9 shows that the field is highest in the middle of the edge, the corners being regions of lower field. This particular field distribution is the reason for the particular pattern found in MO measurements on rectangular samples. The field enhancement is highest in the mid-points of the edges, therefore driving the magnetic field over the critical field first in these points. The four corners meanwhile still remain superconducting. Figure 10 and Figure 11 further illustrate this point.



**Figure 10:** Planar maps of the total magnetic field calculated with OPERA3D below and above the top surface ( $z=1$ ) of the sample ( $5 \times 5 \text{ mm}^2$ , 2 mm thickness).

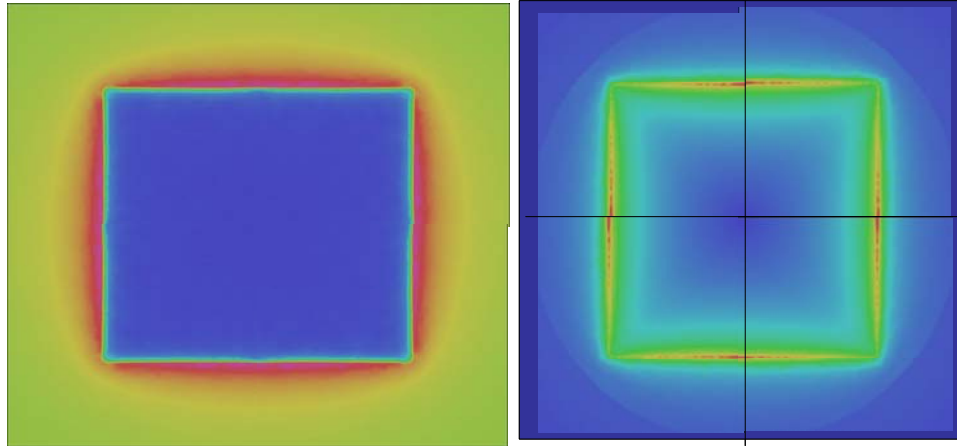


**Figure 11: Calculated field profiles on top of the perfectly superconducting sample. Left: vertical magnetic field ( $B_z$ ), Right: radial magnetic field ( $B_r$ ).**

Figure 12 shows the vertical field across the edges of one quadrant of the superconducting sample. The high field region (white) is concentrated in the mid-points and not in the corner. The figure also shows the x-component of the magnetic field. Generally the x-component arises when the field lines bend around the diamagnetic sample. The x-component is strongest at  $y=0$ , the edge-mid-point.

Figure 13 shows the total field along the x-axis at different heights ( $z$ ) for a perfectly diamagnetic sample ( $5 \times 5 \text{ mm}^2$ ,  $2 \text{ mm}$  thickness). Since the sample is centered in the origin the field peaks at  $x=2.5 \text{ mm}$ , the edge of the  $5 \text{ mm}$  wide sample. As explained above this also happens to be the peak-field point where the field enhancement factor is calculated. The profiles show complete field expulsion inside the sample ( $z < 1 \text{ mm}$ ), and some finite field on top of the sample ( $z > 1 \text{ mm}$ ). As is shown as well this field is mostly oriented in x and y. This can be concluded from the shown  $B_z$  profile above the sample, indicating that

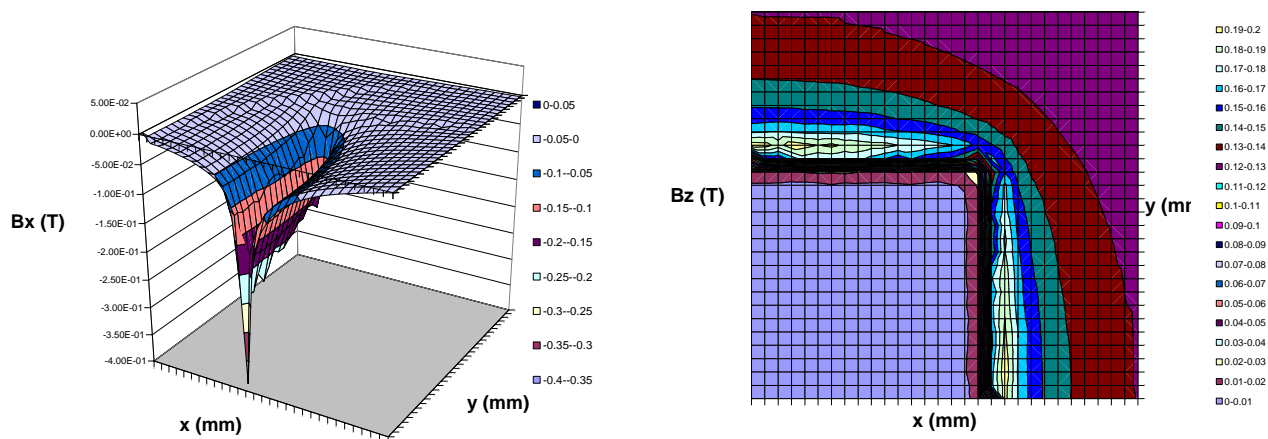


**Figure 12: Magnetic field calculated with OPERA3D,  $10 \mu\text{m}$  above a perfectly superconducting sample ( $5 \times 5 \text{ mm}^2$ ,  $2 \text{ mm}$  thickness) Left:  $B_x$ , Right:  $B_z$ .**

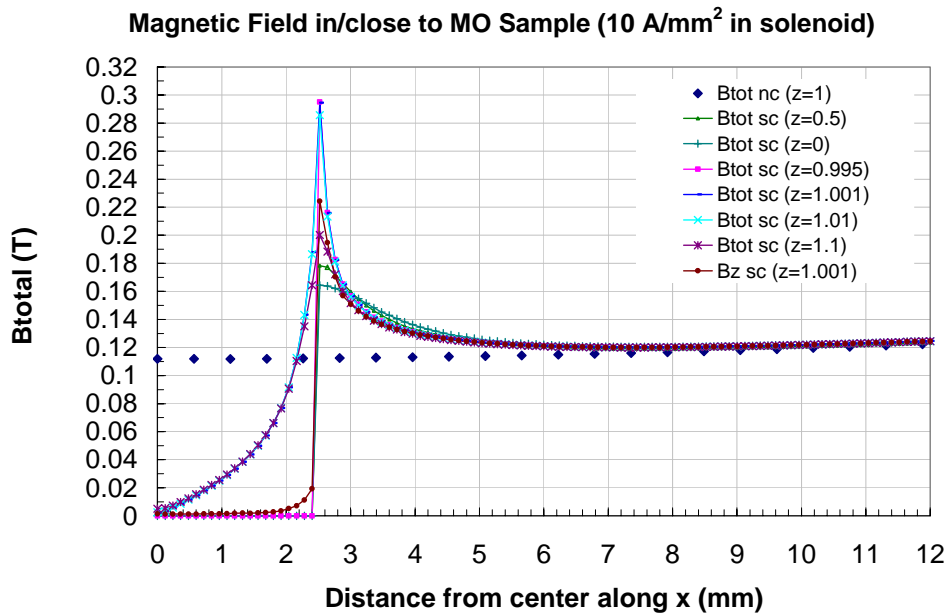


Figure 13: Field profiles calculated with OPERA 3D for a  $5 \times 5$  mm<sup>2</sup>, 2 mm thickness sample.

$B_z$  is essentially zero within the sample. Also shown is the field profile in the absence of the sample. This profile is the reference for the field enhancement factor calculations. As can be approximately derived from the graphs in Figure 13 the field enhancement factors are of the order 2-3. They are clearly highest at the edge of the sample,  $z \sim 1$  mm. Note that the edge is rounded. Figure 14 shows similar field profiles along the diagonal of the

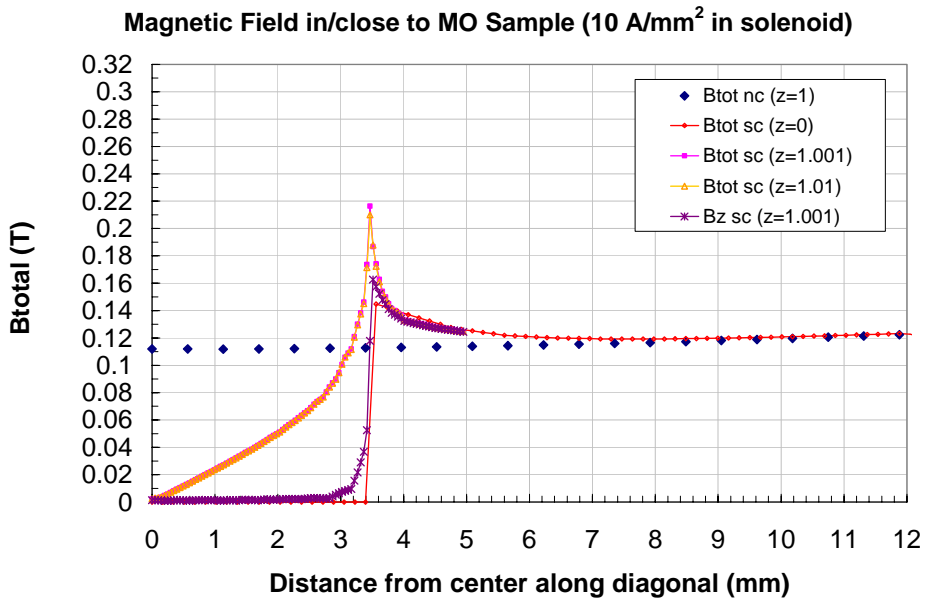


Figure 14: Field profiles calculated with OPERA 3D for a  $5 \times 5$  mm<sup>2</sup>, 2 mm thickness sample.

sample. It becomes clear from this plot that the field enhancement in the sample corner is less pronounced than in the sample edge mid-points.

#### 4) Summary

Figure 15 summarizes the field calculations discussed above to simulate the MO setup at the ASC/UW. The total field profiles just above the sample are shown along  $x$  or  $r$  for a  $5 \times 5 \text{ mm}^2$ ,  $2 \text{ mm}$  thickness sample. To show the agreement the 2D profile is also shown. The agreement between 2D and 3D models with respect to the calculation of the field profile through the mid-edge points of the sample indicates that the 2D model suffices for a systematic calculation of peak field enhancement factors. Figure 17 and Table 1 summarize such a calculation in which the dimensions of a square sample, thickness and width, were varied across the range of interest to the study of SRF Nb conducted at the ASC/UW in collaboration with Fermilab. The field enhancement factors were calculated from the field at the  $(width/2, thickness/2)$  coordinate. This coordinate point is shown in Figure 16. This particular point was chosen because it is well within the “air” region surrounding the sample and therefore less subject to numerical error, typical for interfaces between elements with different material properties. The field enhancement derived here is therefore *not* the peak field enhancement factor, since the highest field concentration occurs at points closer to the sample.

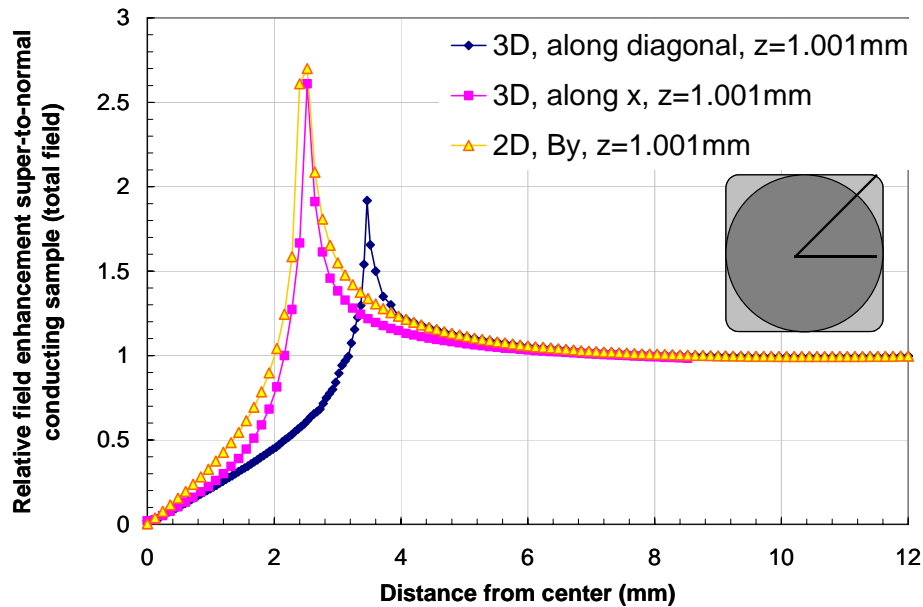


Figure 15: Field profiles calculated with OPERA 2D/3D for a  $5 \times 5 \text{ mm}^2$ ,  $2 \text{ mm}$  thickness sample.

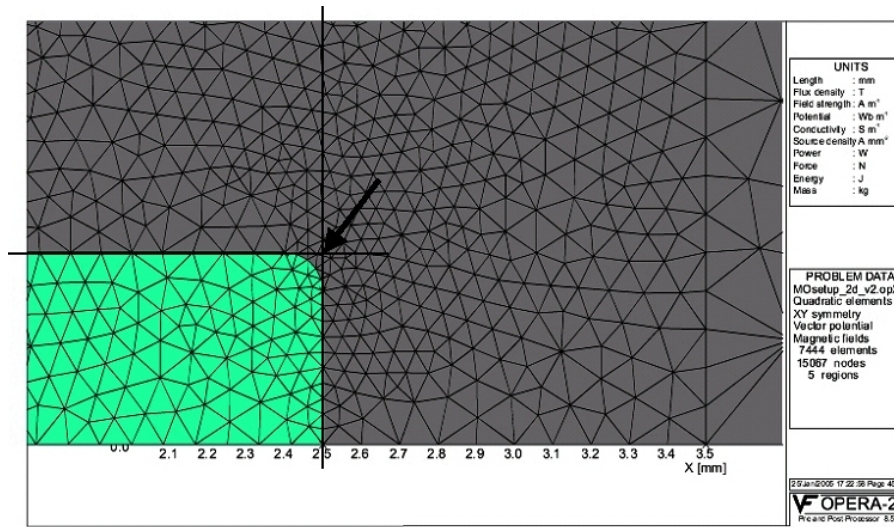


Figure 16: Point at which field enhancement factor was calculated.

Table 1: Peak field enhancement factors calculated for different sample dimensions with OPERA2D.

thick/width	2 mm	3.4 mm	5 mm
0.5 mm	2.3005	2.91325	3.51525
1 mm	2.148925	2.67675	3.17125
1.4 mm	2.0855	2.59075	3.0745
2 mm	2.021	2.4725	2.924
2.6 mm	1.98875	2.4295	2.87025

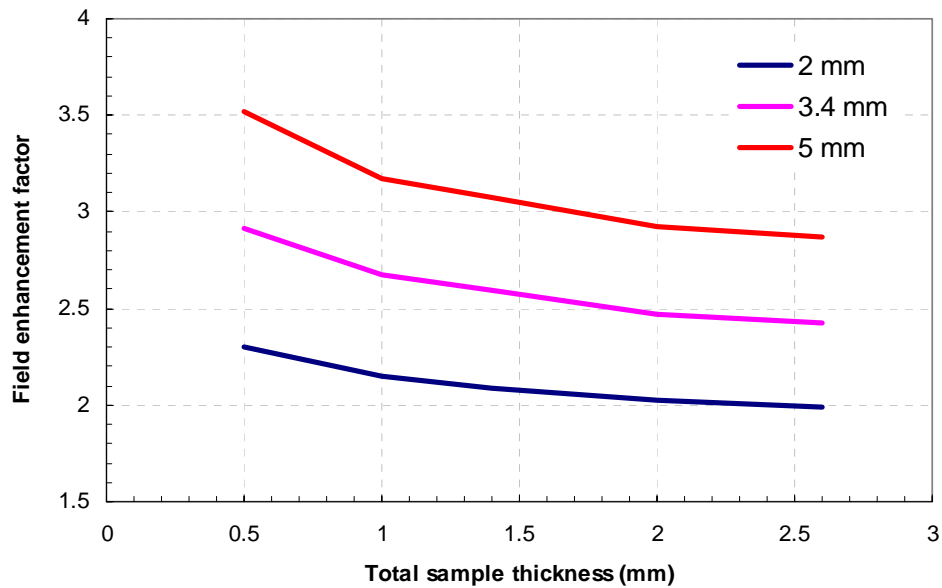


Figure 17: Calculated field enhancement factors for different samples dimensions.

## 5) References

- [1] P. Lee et al., "*An Investigation of the Properties of BCP Niobium for Superconducting RF Cavities*", Proceedings of the "Pushing the Limits of RF Superconductivity" workshop, Argonne National Lab, Sept. 22-24 2004, Chicago, USA
- [2] A. A. Polyanskii, D. M. Feldmann, and D. C. Larbalestier, "*Magneto-Optical Characterization Techniques*", "The Handbook on Superconducting Materials," Edited by David Cardwell and David Ginley, Institute of Physics UK , pp. 1551, 2003.
- [3] Y. Iwasa, "*Case Studies in Superconducting Magnets*", Plenum Press 1994